Contribution of base-pairing interactions between group II intron fragments during *trans*-splicing in vivo

CECILIA QUIROGA, LISA KRONSTAD, CHRISTINE RITLOP, AUDREY FILION, and BENOIT COUSINEAU[1]
Department of Microbiology and Immunology, McGill University, Montréal, Québec, Canada H3A 2B4

ABSTRACT

Group II introns are mobile genetic elements that self-splice from pre-mRNA transcripts. Some fragmented group II introns found in chloroplastic and mitochondrial genomes are able to assemble and splice in *trans*. The Ll.LtrB group II intron from the Gram-positive bacterium *Lactococcus lactis* was shown to splice in *trans* when fragmented at various locations throughout its structure. Here we used Ll.LtrB to assess the contribution of base-pairing interactions between intron fragments during *trans*-splicing in vivo. By comparing closely located fragmentation sites, we show that Ll.LtrB *trans*-splices more efficiently when base-pairing interactions can occur between the two intron fragments. Disruptions and stepwise restorations of specific base-pairing interactions between intron fragments resulted respectively in significant reductions and recoveries of the Ll.LtrB *trans*-splicing efficiency. Finally, although we confirm that LtrA is an important co-factor for *trans*-splicing, its overexpression cannot compensate for the reduction in *trans*-splicing efficiency when the potential base-pairing interactions between intron fragments are disrupted. These findings demonstrate the important contribution of base-pairing interactions for the assembly of group II intron fragments during *trans*-splicing and rationalizes why such interactions were evolutionarily conserved in natural *trans*-splicing group II introns.

Keywords: Ll.LtrB; *Lactococcus lactis*; LtrA; conjugation; sex factor

INTRODUCTION

Group II introns are retromobile elements found in bacteria, bacterial-derived organelles, and archaea (Lambowitz and Zimmerly 2004, 2010). These intervening sequences are RNA enzymes that splice autocatalytically from pre-mRNA transcripts. However, they require the assistance of maturases to fold into their active three-dimensional structure in order to splice in vivo. Despite sharing very little sequence similarity, these large ribozymes fold into a highly conserved RNA secondary structure that consists of six domains (DI to DVI) radiating from a central wheel (e.g., Fig. 1A; Michel et al. 1989; Qin and Pyle 1998; Toor et al. 2001). Each domain contains specific features that contribute to the folding of the intron into its active tertiary conformation. DI, which is the largest domain and the first to be transcribed, provides the scaffold to dock the remaining intron domains. Accordingly, DI takes part in many long-range tertiary interactions with other domains and orchestrates the overall folding of group II introns (Fedorova and Zingler 2007; Pyle et al. 2007). While DII is a small structural domain, DIII functions as a catalytic effector that stimulates splicing (Fedorova et al. 2003). Most group II introns harbor an open reading frame (ORF) in the loop region of DIV that codes for an intron-encoded protein (IEP). IEPs are multifunctional proteins involved in both intron splicing and mobility (Saldanha et al. 1993; Matsuura et al. 2001; Cui et al. 2004). DV is the catalytic domain of group II introns, which positions the catalytic nucleotides and two Mg^{++} ions at the center of the catalytic core (Pyle 2002). Finally, DVI harbors the branch point nucleotide positioned near the 3′ end of the intron (Lambowitz and Zimmerly 2004, 2010). This highly conserved bulged adenosine is also part of the catalytic center since it initiates the splicing reaction.

Group II introns self-splice from pre-mRNA transcripts by two consecutive *trans*-esterification reactions (Fig. 1B, *cis*-splicing; Lambowitz and Zimmerly 2004). Following transcription of the interrupted gene (step 1), the 2′-OH of the bulged adenosine residue in DVI (circled A) initiates the first nucleophilic attack at the exon 1–intron splice junction (step 2) which generates a 2′–5′ linkage. Then, the 3′-OH of the released exon 1 performs the second nucleophilic attack at the intron–exon 2 splice junction (step 3), releasing the

[1]**Corresponding author.**
E-mail benoit.cousineau@mcgill.ca.
Article published online ahead of print. Article and publication date are at http://www.rnajournal.org/cgi/doi/10.1261/rna.028886.111.

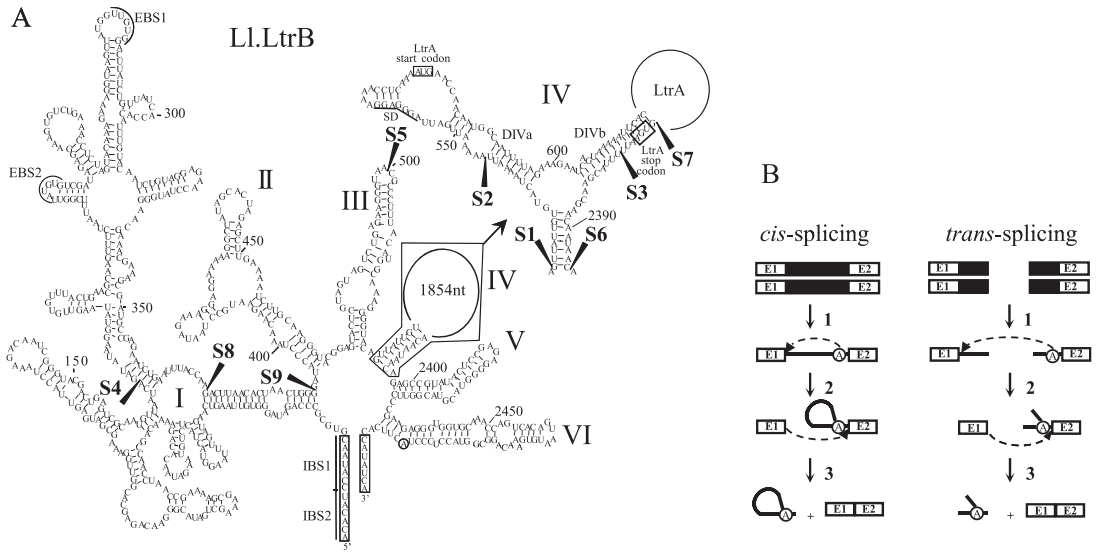

FIGURE 1. Ll.LtrB secondary structure and splicing pathways. (*A*) Ll.LtrB secondary structure. The six domains of Ll.LtrB are indicated (I–VI) and the detailed secondary structure of a portion of domain IV is also shown (*top right*). The *ltrA* start and stop codons are boxed and the Shine–Dalgarno sequence (SD) is underlined. Exons 1 and 2 at both 5′ and 3′ extremities of the intron are also boxed. Fragmentation sites are mapped with black arrowheads (S1–S9). S4 was not used in this study. EBS1 and EBS2, exon-binding site 1 and 2; IBS1 and IBS2, intron-binding site 1 and 2; branch point, circled A. (*B*) Group II intron *cis*- and *trans*-splicing pathways. Following transcription of the interrupted gene (step 1), the 2′-OH of the bulged adenosine present in domain VI (circled A) performs the initial nucleophilic attack at the exon 1–intron splice junction generating a 2′–5′ linkage (step 2). Then, the 3′-OH of the released exon 1 performs the second nucleophilic attack at the intron–exon 2 splice junction, releasing the intron lariat and ligating the flanking exons (step 3). Fragmented group II introns can also splice in *trans* using the same pathway (steps 1–3). Because *trans*-splicing occurs between two independent RNA transcripts, the intron is released as a Y-branched molecule instead of a lariat. Group II intron, black line; exon 1 and 2, E1 and E2; branch point, circled A.

intron lariat and ligating the flanking exons (Lehmann and Schmidt 2003). The intron-free mature mRNA can then be translated and the encoded protein synthesized.

Some group II introns fragmented in two or three pieces have been found in chloroplasts of algae as well as in chloroplasts and mitochondria of higher plants (Glanz and Kuck 2009; and references within). These fragmented introns splice in *trans* using the same pathway as *cis*-splicing introns (Fig. 1B, *trans*-splicing). Following transcription of the separate gene pieces (step 1), the intron fragments presumably assemble and fold into the active tertiary structure allowing the two *trans*-esterification reactions to occur (steps 2 and 3). Because *trans*-splicing takes place between two RNA transcripts, the intron is released as a Y-branched molecule instead of a lariat.

The Ll.LtrB group II intron from the Gram-positive bacterium *Lactococcus lactis* is 2.5 kb in length and encodes for LtrA, a 599-amino acid multifunctional protein with reverse transcriptase, maturase, DNA binding, and endonuclease activities (Mills et al. 1996; Lambowitz and Zimmerly 2004, 2010). LtrA is a very important splicing co-factor for both the *cis*- (Mills et al. 1996; Ichiyanagi et al. 2002; Belhocine et al. 2007) and *trans*-splicing (Belhocine et al. 2007, 2008) of Ll.LtrB in *L. lactis*. It was shown to bind the Ll.LtrB intron RNA at a high affinity-binding site located in DIVa (Wank et al. 1999; Singh et al. 2002) and to multiple secondary sites located in DI, DII, and DVI (Singh et al. 2002; Dai et al. 2008); overall LtrA binds with a 2:1 stoichiometry, suggesting that it may function as a dimer (Saldanha et al. 1999; Rambo and Doudna 2004). Ll.LtrB interrupts the *ltrB* gene, which codes for a relaxase enzyme in three *L. lactis* conjugative elements: the pRS01 and pAH90 plasmids and an integrative and conjugative element called the sex factor (SF) (Mills et al. 1996). The LtrB relaxase is a single-strand endonuclease that nicks the origin of transfer of conjugative elements and initiates their transfer between *L. lactis* strains. Because this enzyme is essential for the initiation of conjugative transfer, splicing of Ll.LtrB is absolutely required for the intercellular transfer of its host elements (Shearman et al. 1996; Klein et al. 2004). Taking advantage of the relationship between the conjugative transfer of the SF and splicing of Ll.LtrB from the relaxase transcript, we developed a highly sensitive *trans*-splicing/conjugation assay in *L. lactis*. Using this assay we demonstrated that Ll.LtrB is able to splice in *trans* when fragmented at natural group II intron fragmentation sites (Belhocine et al. 2007). We also showed that Ll.LtrB *trans*-splices efficiently when fragmented at various other locations throughout its structure, therefore demonstrating the versatility of Ll.LtrB compared to *trans*-splicing group II introns found in nature (Belhocine et al. 2008).

In this study we use the Ll.LtrB group II intron as a model system to assess the contribution of base-pairing interactions between intron fragments during *trans*-splicing

in vivo. Using the *trans*-splicing/conjugation assay that we developed, we observe that Ll.LtrB variants with potential base-pairing interactions between the two intron fragments *trans*-splice more efficiently than variants that are fragmented at close proximity but do not have any potential interactions between the two intron fragments. We also show that abolishing specific base-pairing interactions between intron fragments of Ll.LtrB variants fragmented in DI, DIII, DIVa, or DIVb resulted in important reductions in *trans*-splicing efficiency. Moreover, we demonstrate that stepwise restorations of base-pairing interactions between intron fragments by either the re-establishment of the wild-type sequence or sequence complementarity resulted in significant recovery of the *trans*-splicing efficiency. Finally, although we confirm that LtrA is an important Ll.LtrB *trans*-splicing co-factor, overexpression of LtrA cannot compensate for the reduction in Ll.LtrB *trans*-splicing efficiency when the potential base-pairing interactions between intron fragments are disrupted. Altogether these findings demonstrate the important contribution of base-pairing for the assembly of intron fragments during *trans*-splicing and rationalize why such interactions were evolutionarily conserved between nucleotides located on either side of fragmentation sites in natural *trans*-splicing group II introns.

MATERIALS AND METHODS

Strains and plasmids

The *L. lactis* strains NZ9800Δ*ltrB*::*tet* (Klein et al. 2004) and LM0231 (Shearman et al. 1996) were grown at 30°C without shaking in M17 media (Oxoid) supplemented with 0.5% glucose (GM17). The *Escherichia coli* DH10β strain was used for cloning and was grown at 37°C in LB broth (Wisent) with shaking. When necessary, antibiotics were added at the following concentrations: 3 μg/mL for tetracycline (Tet), 300 μg/mL for spectinomycin (Spc), 25 μg/mL for fusidic acid (Fus), and 10 μg/mL for chloramphenicol (Cam).

Plasmids pDL-P_{23}^2, pDL-P_{23}^2-*ltrB*, pDL-P_{23}^2-S1-WT, pDL-P_{23}^2-S2-WT, pDL-P_{23}^2-S3-WT, and pDL-P_{23}^2-S5-WT were previously engineered (Belhocine et al. 2007). The other fragmented variants of Ll.LtrB (pDL-P_{23}^2-S6-WT to pDL-P_{23}^2-S9-WT) were generated by PCR amplification using the interrupted *ltrB* gene as the template. Each construct was created using two pairs of primers (Supplemental Table S1). The first primer pairs (NotI) were used to amplify the 5′ end of the *ltrB* gene, from the beginning of the 5′ exon up to the respective fragmentation points within the intron. The second primer pairs (BssHII) were used to amplify the region from the fragmentation sites within the intron up to the end of the 3′ exon (Belhocine et al. 2007). Plasmids pDL-P_{23}^2-S1-ΔORF to pDL-P_{23}^2-S9-ΔORF were similarly created but using as the PCR template the *ltrB* gene interrupted by the ΔORF version of Ll.LtrB (Supplemental Table S1).

Plasmids containing different intron variants with disruptions and restorations of base-pairing interactions in DI, DIII, DIVa, and DIVb were engineered either by site-directed mutagenesis or by PCR using the Ll.LtrB ΔORF intron as the template (Supplemental Table S1). Disruptions of the base-pairing interactions were done by replacing G↔C and T↔A. The unpaired nucleotides located between stems were not modified.

The pLE-P_{nis}-*ltrA* plasmid was constructed by first cloning the nisin-inducible promoter (P_{nis}) into the unique BamHI site of the Gram-positive/Gram-negative shuttle plasmid pLE1. The PCR-amplified *ltrA* gene (NotI) was then introduced at the engineered NotI site directly downstream from P_{nis} (Supplemental Table S1). Integrity of all plasmids was confirmed by sequencing (Génome Québec).

Conjugation assay

Mating was done on 5% non-fat dried milk plates (Carnation milk) containing 1% glucose and 1.5% agar. *L. lactis* NZ9800Δ*ltrB*::*tet* (Tet^R) was used as the donor strain while *L. lactis* LM0231 (Fus^R) was used as the recipient strain. Both strains were diluted from saturated overnight cultures (0.4 mL into 10 mL) and grown for 7 h at 30°C. Cells were collected by centrifugation, mixed, spread on milk plates, incubated at 30°C for 16 h, and recovered with PBS 1×. Serial dilutions were plated on GM17 plates containing the specific antibiotic to select for donor, recipient or trans-conjugant cells. Conjugation efficiency of the chromosomal SF was assessed with two different assays (Fig. 2A). The first assay measured the SF conjugation efficiency when LtrA is encoded within the Ll.LtrB intron (pDL-P_{23}^2-Sx-WT series). The second assay determined the SF transfer efficiency when LtrA is provided in *trans* from pLE-P_{23}^2-*ltrA* (pDL-P_{23}^2-Sx-ΔORF series). The conjugation efficiencies were calculated as the ratio of trans-conjugant (Fus^R/Tet^R) to donor cells (Spc for LtrA provided in *cis*, Spc/Cam for LtrA provided in *trans*) for three independent assays.

RNA isolation and qRT-PCR

L. lactis strains containing pLE-P_{nis}-*ltrA* and one of the pDL-P_{23}^2-Sx-ΔORF variant were grown to logarithmic phase (OD_{600} = 0.5), aliquoted, and induced for 3 h with serial dilutions of nisin (Sigma) (0 ng/mL, 0.14 ng/mL, 0.28 ng/mL, 0.42 ng/mL, 0.56 ng/mL, 0.70 ng/mL, 0.84 ng/mL, 0.98 ng/mL). Cell pellets were mixed with 500 mL of TRIzol (Invitrogen life technologies) and 250 mg of acid-washed glass beads (Sigma). The mixture was vortexed for 3 min and incubated at 55°C for 5 min; this treatment was repeated a total of three times. The remainder of the RNA extraction was performed according to the manufacturer's protocol. Total RNA concentration and quality was determined using a NanoDrop 1000 instrument (Thermo Scientific). Total RNA (10 μg) was treated with 2 U of DNAseI (New England Biolabs) for 30 min at 37°C in a final volume of 50 μL and heat-inactivated for 15 min at 75°C in the presence of 5 mM EDTA. Quantitative RT-PCR was performed with ~0.5 μg of treated total RNA using the EXPRESS One-Step SYBR GreenER kit (Invitrogen) and the Rotor Gene RG-3000 software from the Thermo LightCycler instrument (Corbetz Research) (Supplemental Table S1). Amplification conditions were: (95°C, 20 sec; 60°C, 1 min) × 45. Slope noise correction and dynamic tube normalization was applied to the raw fluorescence data prior to analysis. The Ct values recorded during amplification, which correspond to the point at which the level of fluorescence rises significantly above the background, were analyzed. In order to obtain the ΔCt of each sample, we subtracted the level of fluorescence recorded in our negative control to the fluorescence detected for each sample. Inter-run variations were adjusted using as a calibrator

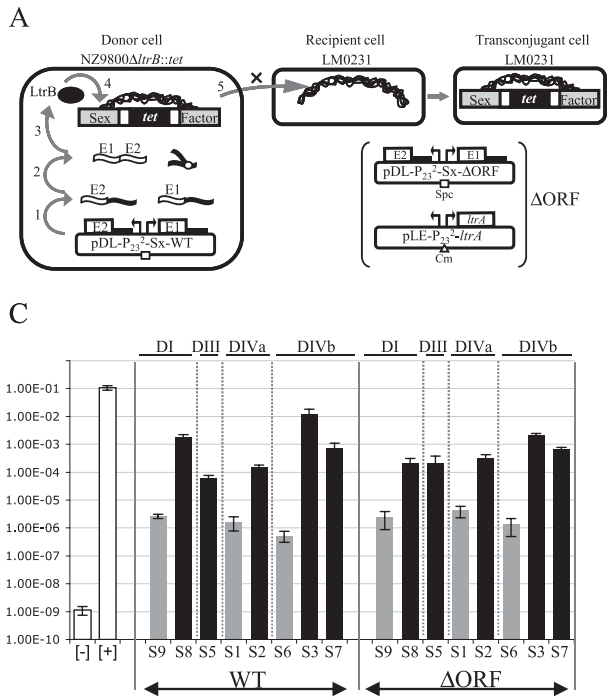

B

Conjugation efficiencies of plasmids harboring various Ll.LtrB variants

Plasmid	C. E.	S. E.
pDL-P_{23}^2	1.13E-09	3.80E-10
pDL- P_{23}^2-*ltrB*	1.08E-01	2.10E-02
pDL- P_{23}^2-S9-WT	2.64E-06	4.72E-07
pDL- P_{23}^2-S8-WT	1.72E-03	5.40E-04
pDL- P_{23}^2-S5-WT[a]	6.03E-05	1.64E-05
pDL- P_{23}^2-S1-WT[a]	1.66E-06	8.80E-07
pDL- P_{23}^2-S2-WT[a]	1.44E-04	3.70E-05
pDL- P_{23}^2-S6-WT	5.29E-07	2.22E-07
pDL- P_{23}^2-S3-WT[a]	1.16E-02	6.40E-03
pDL- P_{23}^2-S7-WT	9.71E-04	2.34E-04
pDL- P_{23}^2-S9-ΔORF	2.39E-06	1.53E-06
pDL- P_{23}^2-S8-ΔORF	2.05E-04	1.03E-04
pDL- P_{23}^2-S5-ΔORF	2.12E-04	1.65E-04
pDL- P_{23}^2-S1-ΔORF	4.15E-06	1.82E-06
pDL- P_{23}^2-S2-ΔORF	3.22E-04	1.07E-04
pDL- P_{23}^2-S6-ΔORF	1.35E-06	8.60E-07
pDL- P_{23}^2-S3-ΔORF	2.05E-03	4.20E-04
pDL- P_{23}^2-S7-ΔORF	6.59E-04	1.12E-04

C.E.; conjugation efficiency
S.E.; standard error
[a] Belhocine *et al*., 2007

FIGURE 2. Ll.LtrB *trans*-splicing/conjugation assay and SF conjugation rates. (*A*) The *trans*-splicing efficiency of Ll.LtrB is monitored by the conjugation rate of the SF between two *L. lactis* strains. The donor cell harbors the chromosomal SF with a defective relaxase gene (NZ9800Δ*ltrB*::*tet*) while the recipient cell lacks the SF (LM0231). The Ll.LtrB intron, along with portions of its exons, was replaced in the chromosome of NZ9800 by a tetracycline resistance marker (*tet*), which prevents expression of the relaxase (LtrB). The LtrB deficient strain is complemented by providing the interrupted *ltrB* gene from a plasmid. Following transcription of the gene pieces (step 1), intron fragments assemble, Ll.LtrB *trans*-splices, and the flanking exons are ligated (step 2). Mature mRNA is translated and leads to expression of the relaxase enzyme (LtrB) (step 3), which recognizes the SF origin of transfer (*oriT*) (step 4) and initiates its transfer from a donor to a recipient cell by conjugation (step 5). Transfer efficiency of conjugative elements between *L. lactis* strains was previously shown to be directly proportional to Ll.LtrB splicing from the relaxase transcript (Klein et al. 2004; Belhocine et al. 2007). In a second version of the assay, the pLE-LtrA plasmid was introduced in various *L. lactis* strains (NZ9800Δ*ltrB*::*tet*/pDL-P_{23}^2-Sx-ΔORF) to provide LtrA in *trans* (between brackets). Ll.LtrB group II intron, black line; exon 1 and 2, E1 and E2; P_{23} promoter, bent arrows; SF, gray; intron RNA fragments, black wavy lines; RNA exons, white wavy lines; LtrB, black oval; spectinomycin resistance marker, Spc; chloramphenicol resistance marker, Cm; *L. lactis* chromosome, scribble. (*B*,*C*) SF conjugation efficiency in the presence of the *ltrB* gene interrupted by various Ll.LtrB fragmented introns (S1–S9 WT and ΔORF). Gray bars, bipartite introns with no potential base-pairing interactions; black bars, bipartite introns with potential base-pairing interactions; white bars, negative ([−], pDL-P_{23}^2, empty vector) and positive ([+], pDL-P_{23}^2-*ltrB*, full length Ll.LtrB) controls.

the pDL-P_{23}^2-S1 variant grown in the absence of nisin. The final fold differences were obtained with the comparative quantification algorithm: $2^{-\Delta\Delta Ct}$, where $\Delta\Delta Ct = (Ct_{ltrB} - Ct_{ldhB})_{sample} - (Ct_{ltrB} - Ct_{ldhB})_{calibrator}$. The values were normalized using the *ldhB* housekeeping gene as a reference (Supplemental Table S1). All assays were performed in triplicate to confirm reproducibility and data presented are the average and standard errors. Specificity of the PCR reaction was analyzed on 2% agarose gel and the PCR product was confirmed by DNA sequencing (Genome Québec).

RESULTS

Ll.LtrB *trans*-splicing efficiency is significantly different between introns fragmented in close proximity in DI, DIII, DIVa, or DIVb

In order to assess the contribution of base-pairing interactions during *trans*-splicing, Ll.LtrB was split in two fragments (Fig. 1A, S1 to S9). Then, *trans*-splicing efficiency was compared between bipartite introns with close fragmentation sites that allowed for or lacked potential base-pairing interactions between the two fragments. Ll.LtrB *trans*-splicing was monitored by measuring the conjugation efficiency of the chromosomal SF between *L. lactis* strains (Fig. 2A; Belhocine et al. 2007). Following transcription of the two gene pieces (step 1), Ll.LtrB *trans*-splices and ligates its flanking exons (step 2). This leads to expression of the relaxase enzyme (LtrB) (step 3), which recognizes the origin of transfer of the SF (step 4) and initiates SF transfer from a donor to a recipient cell by conjugation (step 5). Transfer efficiency of the SF between *L. lactis* strains is directly proportional to Ll.LtrB splicing from the relaxase transcript (Klein et al. 2004; Belhocine et al. 2007).

Fragmentation of Ll.LtrB at position S8 in DI provides a potential interaction of 16 bp between the two intron RNA fragments while fragmentation at position S9, only 18 nt

downstream, does not. Ll.LtrB fragmented at S8 supports conjugative transfer of the SF more efficiently than S9 (Fig. 2B). This is similar to what was previously observed when comparing the *trans*-splicing efficiency of Ll.LtrB fragmented at positions S1 and S2 in DIVa, which are only 19 nt apart. Ll.LtrB fragmented at S2, which allows for a potential interaction of 16 bp between the two intron fragments, *trans*-splices more efficiently than S1, which in contrast does not allow for any potential base-pairing (Fig. 2B; Belhocine et al. 2007). Next, we compared close fragmentation sites in other domains of Ll.LtrB. In accordance with our previous observations in DI and DIVa, Ll.LtrB fragmented at the tip of DIII at position S5 *trans*-splices more efficiently than if the fragmentation site is located 26 nt downstream at position S1 (Fig. 2B). This suggests that the potential interaction of 17 bp between the two RNA fragments contributes to intron assembly during *trans*-splicing in *L. lactis*. Next, we compared the *trans*-splicing efficiency of Ll.LtrB fragmented at position S6, located at the bottom of the stem in DIV, with two intron variants fragmented in DIVb at positions S3 and S7 allowing for potential interactions of 15 and 22 bp, respectively, between the two intron fragments. The Ll.LtrB variants fragmented at positions S3 and S7 were significantly more efficient than S6 (Fig. 2B).

Fragmentation sites located in both DIVa (S1, S2) and DIVb (S3, S6, S7) are adjacent to the extremities of the *ltrA* gene and may affect LtrA expression levels (Fig. 1A). Since LtrA was shown to be a very important splicing co-factor (Mills et al. 1996; Ichiyanagi et al. 2002; Belhocine et al. 2007, 2008), it is crucial to keep its expression level constant while assessing the contribution of base-pairing interactions during *trans*-splicing. In order to ensure comparable levels of LtrA expression for all fragmented intron variants, we modified our *trans*-splicing/conjugation assay by removing most of the LtrA coding region (ΔORF) from the fragmented introns and providing LtrA in *trans* from a second plasmid (pLE-P_{23}^{2}-*ltrA*) (Fig. 2A, ΔORF; Belhocine et al. 2007). The *trans*-splicing efficiencies observed for the ΔORF fragmented introns show the same trend as their wild-type counterparts; that is, the bipartite introns allowing for potential base-pairing interactions between the intron fragments *trans*-splice more efficiently than the variants that do not allow for any interactions (Fig. 2B,C, cf. WT and ΔORF).

Base-pairing interactions between intron fragments contribute to Ll.LtrB *trans*-splicing in *L. lactis*

To further investigate the contribution of base-pairing interactions between intron fragments during *trans*-splicing, we disrupted potential interactions near various engineered fragmentation sites in different domains of Ll.LtrB ΔORF, as well as in the non-fragmented ΔORF *cis*-splicing intron. Next, we performed stepwise restoration of base-pairing interactions by either wild-type sequence restoration or sequence complementarity.

The first fragmentation site investigated was S8 in DI. Site-directed mutagenesis was used to replace the 16 pairing nucleotides at the 5′ end of the second intron fragment with the complementary sequence, abolishing base-pairing inter-

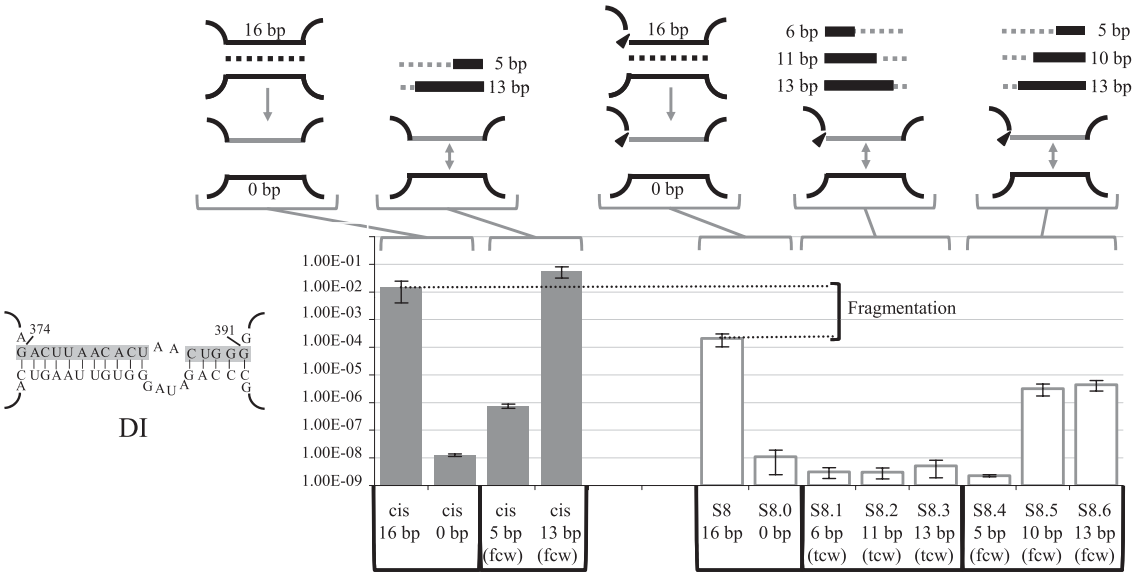

FIGURE 3. Sex factor conjugation efficiency of the Ll.LtrB S8ΔORF variants. Nucleotides modified to abolish base-pairing interactions in S8 and in the *cis*-splicing intron are shown on the *left* (gray box). Schematics of the different *cis*- and *trans*-splicing intron variants are illustrated at the *top* showing the modified RNA strand (gray line). The sequential base pair restorations toward the central wheel (tcw) or from the central wheel (fcw) are identified as gray and black lines while dotted lines depict unpaired residues. The S8 fragmentation site is represented by an arrowhead. Conjugation efficiencies are from three independent assays (Supplemental Table S2).

actions between the two fragments (Fig. 3, S8.0). As a result, *trans*-splicing efficiency dropped by ~19,000-fold. Then, we used two different approaches to sequentially restore the wild-type base-pairing interactions. Stepwise restorations of 6, 11, or 13 bp, directed toward the central wheel (tcw), did not lead to recovery of *trans*-splicing efficiency (Fig. 3, S8.1 to S8.3). In contrast, stepwise restorations starting from the central wheel (fcw) led to partial but significant recovery of the Ll.LtrB *trans*-splicing activity (Fig. 3, S8.4 to S8.6). While a 5-bp restoration was not sufficient to increase *trans*-splicing efficiency, 10- and 13-bp restorations stimulated Ll.LtrB *trans*-splicing by ~300-fold. However, partial restoration of the same stem (fcw) in the *cis*-splicing intron led to complete splicing recovery, indicating that a 13-bp restoration is sufficient to support wild-type splicing efficiency (Fig. 3, *cis* 13 bp). The decreased rescue of splicing in the fragmented intron indicates that even if base-pairing at S8 significantly contributes to Ll.LtrB assembly and *trans*-splicing, fragmentation of the intron at this position also considerably affects the tertiary structure of the ribozyme.

Next, we assessed the contribution of base-pairing interactions during *trans*-splicing of Ll.LtrB fragmented in DIII at position S5. We abolished the 17-bp interaction between the two intron fragments by substituting the pairing residues at the beginning of the second intron fragment for their complementary nucleotides (Fig. 4, S5.0); this led to ~28,000-fold reduction in *trans*-splicing efficiency. We approached restoration of base-pairing in two ways. First, we introduced sequence complementarity at the 3′ end of the first intron fragment, resulting in an inverted stem. Base-pairing interactions were recovered in three consecutive steps moving toward the central wheel (tcw). The Ll.LtrB variant allowing for a 6-bp interaction between fragments did not show any recovery in *trans*-splicing activity (Fig. 4, S5.1), while variants with 11- and 17-bp interactions showed a slight increase in *trans*-splicing efficiency (Fig. 4, S5.2 and S5.3). We also restored the wild-type base pair in three steps from the central wheel (fcw). These variants, allowing for 6-, 11-, and 14-bp interactions, showed a slight increase in *trans*-splicing activity similar to S5.2 and S5.3 (Fig. 4, S5.4 to S5.6). On the other hand, partial restoration of the base-pairing interactions in the *cis* intron led to complete splicing recovery (Fig. 4, *cis* 14 bp). This indicates that base-pairing at S5 significantly contributes to Ll.LtrB assembly during *trans*-splicing. However, similar to what was observed in DI, fragmentation of Ll.LtrB at the tip of DIII may affect the tertiary structure of the ribozyme.

The contribution of base-pairing between intron fragments during Ll.LtrB *trans*-splicing was also analyzed in DIV. We first abolished the potential interactions of 15 bp in DIVb at position S3 by replacing the pairing residues at the beginning of the second intron fragment with their complementary nucleotides (Fig. 5, S3.0). Removing base-pairing between the two intron RNA fragments reduced the *trans*-splicing efficiency of Ll.LtrB by ~2,300-fold. Subsequent stepwise restoration of base-pairing interactions from the central wheel (fcw) was done in four consecutive steps, by sequence complementation of residues within the first intron fragment (Fig. 5, S3.1 to S3.4); this resulted in an inverted stem. While a 4-bp interaction between the two

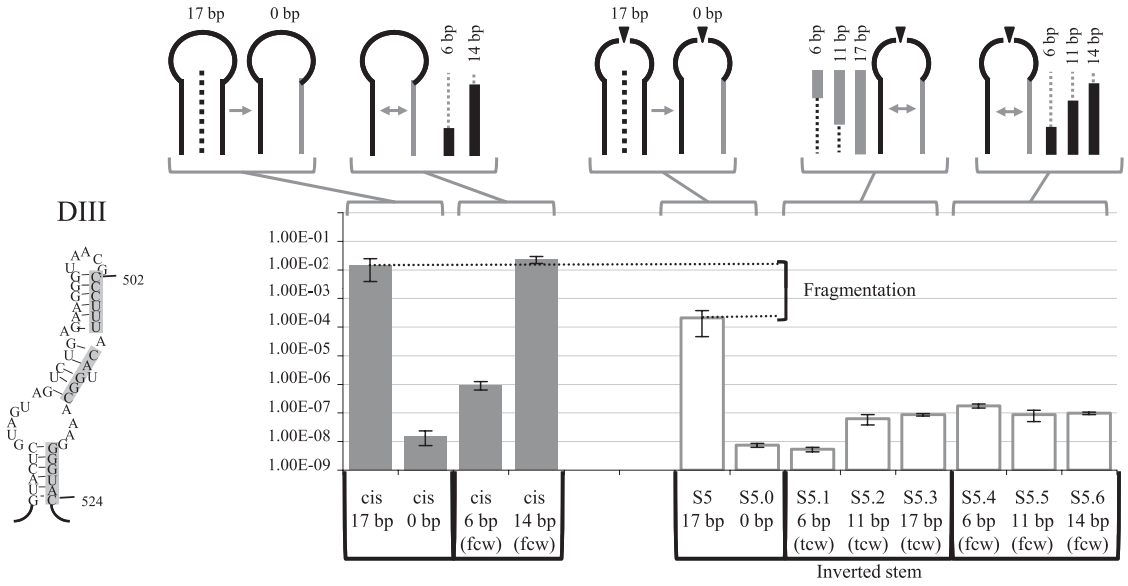

FIGURE 4. Sex factor conjugation efficiency of the Ll.LtrB S5ΔORF variants. Nucleotides modified to abolish base-pairing interactions in S5 and in the *cis*-splicing intron are shown on the *left* (gray box). Schematics of the different *cis*- and *trans*-splicing intron variants are illustrated at the *top* showing the modified RNA strand (gray line). The sequential base pair restorations toward the central wheel (tcw) or from the central wheel (fcw) are identified as gray and black lines while dotted lines depict unpaired residues. The S5 fragmentation site is represented by an arrowhead. Conjugation efficiencies are from three independent assays (Supplemental Table S2).

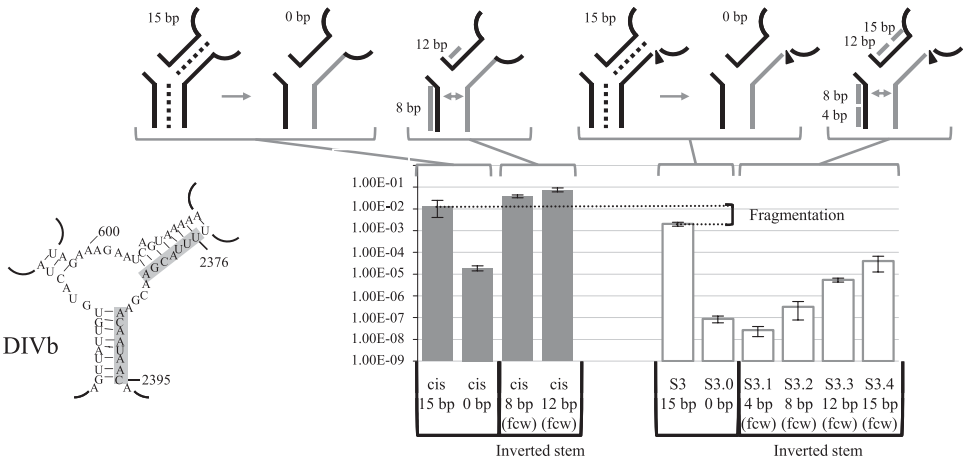

FIGURE 5. Sex factor conjugation efficiency of the Ll.LtrB S3ΔORF variants. Nucleotides modified to abolish base-pairing interactions in S3 and in the *cis*-splicing intron are shown on the *left* (gray box). Schematics of the different *cis*- and *trans*-splicing intron variants are illustrated at the *top* showing the modified RNA strand (gray line). The sequential base pair restorations from the central wheel (fcw) are identified as gray lines. The S3 fragmentation site is represented by an arrowhead. Conjugation efficiencies are from three independent assays (Supplemental Table S2).

intron fragments was not sufficient to recover *trans*-splicing activity, the restoration of 8-, 12-, and 15-bp interactions gradually increased Ll.LtrB *trans*-splicing efficiency by ~3.6-fold, ~63-fold, and ~456-fold, respectively. As observed in DI and DIII, *cis*-splicing is completely recovered when the stem is partially restored by complementation (Fig. 5, *cis* 8 and 12 bp), indicating that even if base-pairing significantly contributes to Ll.LtrB assembly and *trans*-splicing, fragmentation of the intron at S3 seems to also affect the tertiary structure of the ribozyme.

In order to disrupt the base-pairing interaction between the two intron RNAs of Ll.LtrB fragmented at position S2 in DIVa, we replaced the pairing residues at the end of the first intron fragment with their complementary nucleotides (Fig. 6, S2.0). Abolishment of the potential base-pairing interaction between intron fragments again resulted in a significant drop in *trans*-splicing efficiency of ~2,700-fold. This potential interaction between the two intron fragments was then restored by stepwise complementation going toward the central wheel (tcw), resulting in an inverted stem. Residues from the second intron fragment were modified 4 nt at a time (Fig. 6, S2.1 to S2.4). Restoration of 4 bp did not improve Ll.LtrB *trans*-splicing efficiency (Fig. 6, S2.1). However, restoration of 8-, 12-, and 16-bp interactions between the two intron fragments led to a gradual recovery of the Ll.LtrB *trans*-splicing activity of ~8.5-fold, ~340-fold, and ~2050-fold, respectively (Fig. 6, S2.2 to S2.4). Strikingly, restoration of the 16-bp interactions by complementation resulted in complete recovery of the *trans*-splicing activity (Fig. 6, cf. S2 and S2.4) while 12 bp were not sufficient to completely restore the *cis*-splicing activity (Fig. 6, *cis* 12 bp). This indicates that base-pairing at S2 contributes significantly to Ll.LtrB assembly and *trans*-splicing, and that unlike what was observed at S3, S5, and S8, fragmentation of the intron at this position does not strongly affect the tertiary structure of the intron.

Influence of the LtrA protein during Ll.LtrB *trans*-splicing

LtrA is an important splicing co-factor (Mills et al. 1996; Ichiyanagi et al. 2002; Belhocine et al. 2007) that binds to Ll.LtrB at a high affinity-binding site in DIVa (Wank et al. 1999; Singh et al. 2002) and to multiple secondary sites located in DI, DII, and DVI (Singh et al. 2002; Dai et al. 2008). We thus wanted to address the role of this protein in the assembly and folding of Ll.LtrB intron fragments in vivo and its relative importance compared to base-pairing interactions during *trans*-splicing.

In the *trans*-splicing/conjugation assay used above (Fig. 2A, ΔORF), LtrA was expressed at a constant level from the P_{23} constitutive promoter (pLE-$P_{23}{}^{2}$-*ltrA*), independently from the two intron fragments. In order to control the expression level of LtrA, the *ltrA* gene was cloned in pLE downstream from the nisin inducible promoter (pLE-P_{nis}-*ltrA*). Western blots were used to identify the nisin concentration at which LtrA expression levels plateaued in *L. lactis*. The levels of LtrA linearly increased between 0 and 1 ng/mL of nisin and stayed constant at higher nisin concentrations (Supplemental Fig. S1).

To evaluate the importance of LtrA during Ll.LtrB *trans*-splicing, we co-transformed the pLE-P_{nis}-*ltrA* plasmid in *L. lactis* with plasmids containing various bipartite introns fragmented at position S2 and harboring different potential base-pairing interactions between the two intron fragments (Fig. 7, S2.0 to S2.4 and S2). Ll.LtrB *trans*-splicing efficiency was evaluated by monitoring the presence of ligated exons by qRT-PCR at 10 different nisin concentrations ranging from 0 to 0.98 ng/mL (Fig. 7B).

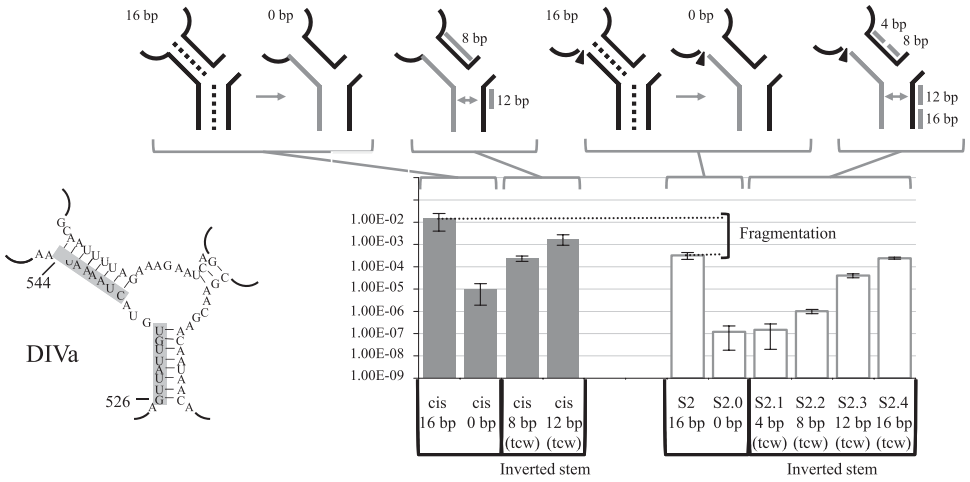

FIGURE 6. Sex factor conjugation efficiency of the Ll.LtrB S2ΔORF variants. Nucleotides modified to abolish base-pairing interactions in S2 and in the *cis*-splicing intron are shown on the *left* (gray box). Schematics of the different *cis*- and *trans*-splicing intron variants are illustrated at the *top* showing the modified RNA strand (gray line). The sequential base pair restorations toward the central wheel (tcw) are identified as gray lines. The S2 fragmentation site is represented by an arrowhead. Conjugation efficiencies are from three independent assays (Supplemental Table S2).

Despite the gradual increase in LtrA levels, no significant differences in *trans*-splicing efficiency is observed above 0.14 ng/mL of nisin, regardless of the number of base pairs between the two intron fragments (Fig. 7B). Further, the maximum level of *trans*-splicing obtained for each variant was proportional to the number of base pairs between the two intron fragments. All constructs showed a residual *trans*-splicing activity in the absence of nisin, suggesting that the nisin promoter is leaky and that small amounts of LtrA are produced under non-induced conditions (Fig. 7, black bars). Residual *trans*-splicing activity under non-induced conditions also increased proportionally with the number of base pairs between the two intron fragments.

DISCUSSION

In this study, we used the Ll.LtrB group II intron as a model to assess the contribution of base-pairing interactions between intron fragments during *trans*-splicing in vivo. Using a *trans*-splicing/conjugation assay that provides LtrA either in *cis* (WT) or in *trans* (ΔORF), we found that bipartite Ll.LtrB variants with the potential for base-pairing between the two intron fragments *trans*-splice more efficiently than variants fragmented at close proximity, but lack the potential to base-pair. Interestingly, we observed this trend across four different locations throughout the intron structure: DI (S8 vs. S9), DIII (S5 vs. S1), DIVa (S2 vs. S1), and DIVb (S3 vs. S6 and S3 vs. S7) (Fig. 2, WT and ΔORF). This suggests that base-pairing interactions between intron fragments are involved during intron assembly and *trans*-splicing in vivo. However, the *trans*-splicing introns lacking base-pairing interactions are fragmented in the central wheel (Fig. 1A, S1, S6, and S9). Since the positions of

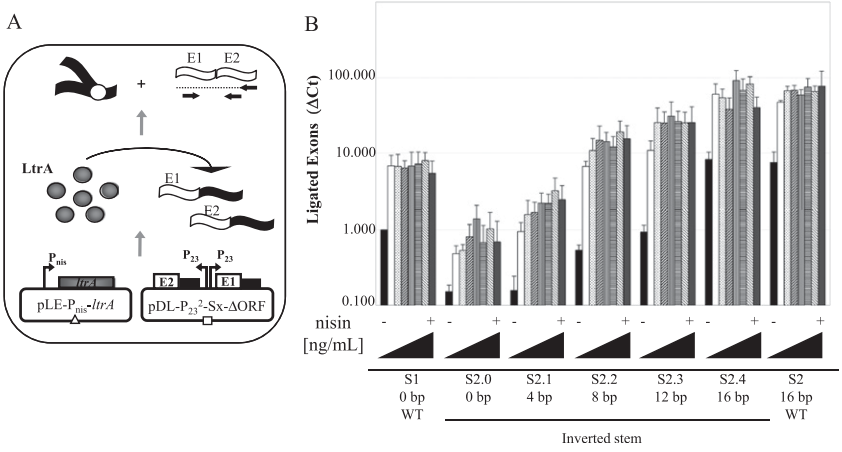

FIGURE 7. Influence of LtrA levels on Ll.LtrB *trans*-splicing in *L. lactis*. (*A*) Ll.LtrB *trans*-splicing efficiency was assessed in the presence of various levels of LtrA by monitoring the level of ligated exons by quantitative RT-PCR. LtrA expression was under the control of the P_{nis} promoter (pLE-P_{nis}-*ltrA*). (*B*) Levels of ligated exon were compared amongst introns having different number of base pairs between the two intron fragments (S2.0ΔORF to S2.4ΔORF, S2ΔORF, S1ΔORF). Ll.LtrB *trans*-splicing efficiency was assessed in the presence of different levels of LtrA expressed from the nisin inducible promoter: black, 0 ng/mL nisin; white, 0.14 ng/mL; dotted, 0.28 ng/mL; upward diagonals, 0.42 ng/mL; vertical lines, 0.56 ng/mL; horizontal lines, 0.70 ng/mL; downward diagonals, 0.84 ng/mL; gray, 0.98 ng/mL. Exon 1 and exon 2, E1 and E2; Ll.LtrB variants, black lines; *ltrA* gene, gray box; P_{23} and P_{nis} promoters, bent arrows; Ll.LtrB RNA intron fragments, black wavy lines; RNA exons, white wavy lines; LtrA, gray circles; primers used for the qRT-PCR, horizontal arrows.

these fragmentation sites are between residues that lie close to the catalytic center and that are most likely involved in multiple tertiary interactions (Dai et al. 2008; Toor et al. 2010), structural defects probably also contributed to the observed decrease in *trans*-splicing efficiency.

To further investigate the potential contribution and importance of base-pairing interactions between intron RNA fragments during *trans*-splicing, we introduced mutations to disrupt base-pairing interactions at various fragmentation sites in different domains of Ll.LtrB. The abolishment of specific base-pairing interactions between intron fragments of Ll.LtrB variants fragmented in DI (Fig. 3, S8), DIII (Fig. 4, S5), DIVb (Fig. 5, S3), or DIVa (Fig. 6, S2) led to significant reductions in *trans*-splicing efficiency. In all tested domains, disruption of base-pairing was more deleterious than intron fragmentation at positions nearby within the central wheel that do not allow for base-pairing interactions. This further suggests a significant contribution of base-pairing interactions between intron fragments during *trans*-splicing.

Next, we demonstrated that stepwise restorations of base-pairing interactions between intron fragments by either wild-type sequence re-establishment at DI and DIII or sequence complementarity at DIII, DIVa, and DIVb led to significant *trans*-splicing recovery. Complementation in DIVa and DIVb led to complete or nearly complete recovery of *trans*-splicing efficiencies, while base pair restoration in DI and DIII led to partial but significant *trans*-splicing recovery. This suggests that base-pairing interactions are contributing to intron assembly but that other factors have been affected by the engineered fragmentations and nucleotide substitutions. Indeed, some of the nucleotides substituted in DI and DIII are known to be involved in long-range tertiary interactions (Singh et al. 2002; Dai et al. 2008). In vitro studies suggest that G374 interacts with G37, helping the intron to fold into its native structure by positioning DIc1 and DIa along a helical turn of DI(ii) (Dai et al. 2008). Similarly in DIII, long-range interactions involving residues G494, C500, G501, and A523 were also shown to be involved in the three-dimensional folding of the intron (Dai et al. 2008). Disruption of these tertiary interactions most likely affected the final ribozyme structure and may explain why *trans*-splicing was only partially recovered in DI and DIII. In contrast, *trans*-splicing gradually increased as base-pairing interactions were progressively restored by complementation in both DIVa and DIVb. While base pair restorations by complementation in DIVb led to high *trans*-splicing efficiency, base pair restoration by complementation in DIVa resulted in complete *trans*-splicing recovery. The important recovery of Ll.LtrB *trans*-splicing activity by sequence complementarity in DIVa toward the central wheel and DIVb from the central wheel indicates that base-pairing interactions are contributing significantly, in a sequence independent manner, to intron fragment assembly. Accordingly, the modified residues in DIVa and DIVb do not appear to be involved in any long-range tertiary interactions (Singh et al. 2002; Dai et al. 2008).

The IEP LtrA is a very important Ll.LtrB splicing co-factor that binds to multiple sites located throughout the intron (Mills et al. 1996; Ichiyanagi et al. 2002; Belhocine et al. 2007, 2008). We thus wanted to address the role of LtrA in the assembly of Ll.LtrB intron fragments and its relative importance compared to base-pairing interactions during *trans*-splicing. The *trans*-splicing efficiency of Ll.LtrB variants fragmented at position S2 was assessed by qRT-PCR in the presence of increasing amounts of LtrA (Fig. 7). The *trans*-splicing efficiency of Ll.LtrB plateaued rapidly at low concentrations of LtrA regardless of the number of base pairs between the two intron fragments. Interestingly, the results obtained by qRT-PCR are consistent with our conjugation data. First, abolishment of the potential base-pairing interactions between the two intron fragments significantly decreased *trans*-splicing efficiency (Figs. 6, 7, cf. S2 and S2.0). Second, *trans*-splicing efficiency of the Ll.LtrB variant fragmented at position S1 (0 bp) is intermediate between S2 (16 bp) and S2.0 (0 bp) (Figs. 7, 2, cf. S1 and S2 and S2.0). Finally, stepwise restoration of the potential base-pairing interactions resulted in a gradual increase of the Ll.LtrB *trans*-splicing efficiency, ultimately reaching complete recovery (Figs. 6, 7, cf. S2 and S2.0 to S2.4). We thus confirmed that LtrA is an important Ll.LtrB *trans*-splicing co-factor in vivo, which allows each Ll.LtrB variant to reach its maximal *trans*-splicing potential. However, we also showed that overexpression of LtrA cannot compensate for the *trans*-splicing deficiencies induced by altering the potential base-pairing interactions between the two intron fragments.

In nature, some chloroplastic and mitochondrial genomes harbor *trans*-splicing group II introns fragmented into two or three pieces (Lambowitz and Zimmerly 2004; Glanz and Kuck 2009). Regardless of the position of the fragmentation site(s), these introns can still be folded into the conserved secondary structure (e.g., Fig. 1A). Analysis of the secondary structures of six chloroplastic (psaA-i1, psaA-i2, petD-i1, psaC-i1, rbcL-i1, rbcL-i2) and six mitochondrial (nad1-i1, nad2-i2, nad5-i3, nad1-i4, nad3-i1, nad3-i2) fragmented group II introns showed that even if the secondary structures were not always perfectly conserved in the vicinity of the fragmentation sites, these fragmented introns have a series of five to 20 potential base-pairing interactions between nucleotides located on either side of the fragmentation sites (Supplemental Table S3). The conservation of these potential base-pairing interactions between intron RNA fragments suggests that they were maintained because they contribute to intron fragment assembly during *trans*-splicing in vivo.

Taken together our data show the important contribution of base-pairing interactions for the assembly of intron fragments during *trans*-splicing in vivo even though other factors, such as long-range tertiary interactions, seem to also play a significant role. Our work also rationalizes why base-pairing interactions were evolutionarily conserved

between nucleotides located on either side of fragmentation sites in natural *trans*-splicing group II introns.

SUPPLEMENTAL MATERIAL

Supplemental material is available for this article.

ACKNOWLEDGMENTS

We thank Lauren Narcross and Dr. Karen K. Yam for providing comments on the manuscript. This work was supported by the Natural Sciences and Engineering Research Council of Canada (NSERC) (#227826 to B.C.). B.C. is a McGill University William Dawson Scholar and a Chercheur-Boursier Senoir from Fonds de la Recherche en Santé du Québec (FRSQ). C.Q. was the recipient of an external post-doctoral fellowship from Consejo Nacional de Investigaciones Cientfícas y Técnicas from Argentina (CONICET). A.F. was the recipient of an Undergraduate Summer Research Award from FRSQ.

Received June 23, 2011; accepted September 8, 2011.

REFERENCES

Belhocine K, Mak AB, Cousineau B. 2007. *Trans*-splicing of the Ll.LtrB group II intron in *Lactococcus lactis*. *Nucleic Acids Res* **35:** 2257–2268.

Belhocine K, Mak AB, Cousineau B. 2008. *Trans*-splicing versatility of the Ll.LtrB group II intron. *RNA* **14:** 1782–1790.

Cui X, Matsuura M, Wang Q, Ma H, Lambowitz AM. 2004. A group II intron-encoded maturase functions preferentially in *cis* and requires both the reverse transcriptase and X domains to promote RNA splicing. *J Mol Biol* **340:** 211–231.

Dai L, Chai D, Gu SQ, Gabel J, Noskov SY, Blocker FJ, Lambowitz AM, Zimmerly S. 2008. A three-dimensional model of a group II intron RNA and its interaction with the intron-encoded reverse transcriptase. *Mol Cell* **30:** 472–485.

Fedorova O, Zingler N. 2007. Group II introns: Structure, folding and splicing mechanism. *Biol Chem* **388:** 665–678.

Fedorova O, Mitros T, Pyle AM. 2003. Domains 2 and 3 interact to form critical elements of the group II intron active site. *J Mol Biol* **330:** 197–209.

Glanz S, Kuck U. 2009. *Trans*-splicing of organelle introns—a detour to continuous RNAs. *Bioessays* **31:** 921–934.

Ichiyanagi K, Beauregard A, Lawrence S, Smith D, Cousineau B, Belfort M. 2002. Retrotransposition of the Ll.LtrB group II intron proceeds predominantly via reverse splicing into DNA targets. *Mol Microbiol* **46:** 1259–1272.

Klein JR, Chen Y, Manias DA, Zhuo J, Zhou L, Peebles CL, Dunny GM. 2004. A conjugation-based system for genetic analysis of group II intron splicing in *Lactococcus lactis*. *J Bacteriol* **186:** 1991–1998.

Lambowitz AM, Zimmerly S. 2004. Mobile group II introns. *Annu Rev Genet* **38:** 1–35.

Lambowitz AM, Zimmerly S. 2010. Group II introns: Mobile ribozymes that invade DNA. *Cold Spring Harb Perspect Biol* doi: 10.1101/cshperspect.a003616.

Lehmann K, Schmidt U. 2003. Group II introns: Structure and catalytic versatility of large natural ribozymes. *Crit Rev Biochem Mol Biol* **38:** 249–303.

Matsuura M, Noah JW, Lambowitz AM. 2001. Mechanism of maturase-promoted group II intron splicing. *EMBO J* **20:** 7259–7270.

Michel F, Umesono K, Ozeki H. 1989. Comparative and functional anatomy of group II catalytic introns—a review. *Gene* **82:** 5–30.

Mills DA, McKay LL, Dunny GM. 1996. Splicing of a group II intron involved in the conjugative transfer of pRS01 in lactococci. *J Bacteriol* **178:** 3531–3538.

Pyle AM. 2002. Metal ions in the structure and function of RNA. *J Biol Inorg Chem* **7:** 679–690.

Pyle AM, Fedorova O, Waldsich C. 2007. Folding of group II introns: A model system for large, multidomain RNAs? *Trends Biochem Sci* **32:** 138–145.

Qin PZ, Pyle AM. 1998. The architectural organization and mechanistic function of group II intron structural elements. *Curr Opin Struct Biol* **8:** 301–308.

Rambo RP, Doudna JA. 2004. Assembly of an active group II intron-maturase complex by protein dimerization. *Biochemistry* **43:** 6486–6497.

Saldanha R, Mohr G, Belfort M, Lambowitz AM. 1993. Group I and group II introns. *FASEB J* **7:** 15–24.

Saldanha R, Chen B, Wank H, Matsuura M, Edwards J, Lambowitz AM. 1999. RNA and protein catalysis in group II intron splicing and mobility reactions using purified components. *Biochemistry* **38:** 9069–9083.

Shearman C, Godon JJ, Gasson M. 1996. Splicing of a group II intron in a functional transfer gene of *Lactococcus lactis*. *Mol Microbiol* **21:** 45–53.

Singh RN, Saldanha RJ, D'Souza LM, Lambowitz AM. 2002. Binding of a group II intron-encoded reverse transcriptase/maturase to its high affinity intron RNA binding site involves sequence-specific recognition and autoregulates translation. *J Mol Biol* **318:** 287–303.

Toor N, Hausner G, Zimmerly S. 2001. Coevolution of group II intron RNA structures with their intron-encoded reverse transcriptases. *RNA* **7:** 1142–1152.

Toor N, Keating KS, Fedorova O, Rajashankar K, Wang J, Pyle AM. 2010. Tertiary architecture of the *Oceanobacillus iheyensis* group II intron. *RNA* **16:** 57–69.

Wank H, SanFilippo J, Singh RN, Matsuura M, Lambowitz AM. 1999. A reverse transcriptase/maturase promotes splicing by binding at its own coding segment in a group II intron RNA. *Mol Cell* **4:** 239–250.